Corrections to the electroweak effective action at finite temperature

C. Glenn Boyd*
Enrico Fermi Institute, 5640 Ellis Avenue, Chicago, Illinois 60637

David E. Brahm†
California Institute of Technology, Mail Code 452-48, Pasadena, California 91125

Stephen D. H. Hsu‡
Lyman Laboratory of Physics, Harvard University, Cambridge, Massachusetts 02138
(Received 28 September 1992)

We calculate contributions to the finite temperature effective action for the electroweak phase transition (EWPT) at $O(g^4)$, i.e., at second order in $(g^2T/\mathcal{M})$ and all orders in $(g^2T^2/\mathcal{M}^2)$. This requires plasma-mass corrections in the calculation of the effective potential, the inclusion of the "lollipop" diagram, and an estimate of derivative corrections. We find the EWPT remains too weakly first order to drive baryogenesis. We calculate some one-loop kinetic energy corrections using both functional and diagrammatic methods; these may be important for saddle point configurations such as the bounce or sphaleron.

PACS number(s): 11.15.Ex, 05.70.Fh, 12.15.Ji, 98.80.Cq

I. INTRODUCTION

Recent work [1,2] suggests the baryon asymmetry may have been generated at the electroweak phase transition (EWPT). This would require the transition be first order [3,4], with the resulting Higgs vacuum expectation value (VEV) large [roughly, $\phi_+(T_b)/T_b > 1.4$]. Several authors [1,5], using the one-loop finite temperature effective potential [6–9], have concluded that these requirements may be met in the standard model (with augmented *CP* violation) for a sufficiently light Higgs boson, say $M_h < 55$ GeV (now just below experimental limits [10]).

Since the transition is weakly first order, infrared divergences [11] from the resultant nearly massless scalar and gauge boson modes make higher-loop graphs important. The inclusion of plasma masses [12] accounts for the most important corrections, $O(g^2T^2/\mathcal{M}^2)$, while all other higher-loop correction are $O(g^2T/\mathcal{M})$ [13]. Several authors have examined plasma mass corrections in the gauge sector [13–16]; while we will refine these calculations, the basic result holds that electric modes decouple [16], reducing the cubic term in V by 1/3. For the Higgs sector, Carrington [15] computed the leading plasma masses [$O(g^2T^2)$ and $O(\lambda T^2)$], and Brahm and Hsu [13] worked to higher order in g. Unfortunately, the vacuum-to-vacuum method we used overcounts some contributions, as pointed out by the authors of Ref. [16] and by Boyd; in this paper we reexamine the Higgs sector using tadpole graphs.

One may question the validity of inserting zero-momentum plasma masses into our diagrams [17]; we estimate the error involved using the derivative expansion of the effective action [18], and also by direct calculation of a two-point graph. We note derivative terms can be important for determining critical bubbles or $(B+L)$-violating sphaleron solutions [19], and resolving questions of gauge invariance.

II. THE ONE-LOOP EFFECTIVE POTENTIAL

The effective action $\Gamma[\bar{\phi}]$ is the double Legendre transform of the generator of one particle irreducible (1PI) truncated Green's functions, and is the Legendre transform of $W[J]$:

$$\Gamma[\bar{\phi}] = W[J] - \int d^4x\, J(x)\bar{\phi}(x)\ , \tag{2.1}$$

where $\bar{\phi}$ is the expectation value of the field operator $\hat{\phi}$ in the presence of source J. The quantum theory described by $W[J]$ is equivalent to a classical (tree-level) theory described by $\Gamma[\bar{\phi}]$, which can be expanded in derivatives:

$$\Gamma[\bar{\phi}] = \int d^4x\,[-V(\phi) + A(\partial_\mu\bar{\phi})^2 + \cdots]\ . \tag{2.2}$$

On the restricted Hilbert space of states localized in ϕ, V is the usual effective potential [20,21].

At finite (nonzero) temperature, V can be identified with the free-energy density in the convex region, and can be calculated by imposing periodic (antiperiodic) boundary conditions on bosonic (fermionic) fields in Euclidean time: $k_4^2 \to \omega_n^2 = (2\pi nT)^2$ and

$$\int [d^4k/(2\pi)^4] \to T\sum_n \int [d^3\mathbf{k}/(2\pi)^3]\ ,$$

where n is an integer (half-integer) for bosons (fermions) [6–8,22,23]. V calculated to one-loop can be written as the sum of tree-level, $T=0$, and finite-T contributions:

*Electronic address: boyd@rabi.uchicago.edu
†Electronic address: brahm@theory3.caltech.edu
‡Electronic address: hsu@hsunext.harvard.edu

$$V=V_0+V_1+V_T\ ,\quad V_0(\phi)=\frac{\lambda}{4}(\phi^2-v^2)^2\ , \tag{2.3}$$

where $\lambda=M_h^2/2v^2$. At any order, a useful approximate parametrization [5,16] is

$$V=D(T^2-T_0^2)\bar{\phi}^2-ET\bar{\phi}^3+\frac{\lambda_T}{4}\bar{\phi}^4\ , \tag{2.4}$$

where T_0 is the temperature at which $V''(\bar{\phi}=0)$ vanishes. This parametrization can be used to estimate quantities such as T_c, the temperature at which there are two degenerate minima, and $\bar{\phi}_+$, the position of the nonsymmetric degenerate minimum.

We add counterterms [5] to V_1 to maintain $V'(v)=0$ and $V''(v)=M_h^2-\Sigma(M_h^2)+\Sigma(0)$ at $T=0$. The latter relation arises because V is calculated at vanishing external momentum while the physical Higgs boson mass is defined on shell ($p^2=M_h^2$) [24]; it is accounted for by "running" λ down to zero momentum:

$$V_1=\frac{\Delta\lambda}{4}(\bar{\phi}^2-v^2)^2 + \sum_j \frac{\pm g_j}{64\pi^2}\left\{m_j^4\ln\left[\frac{m_j^2}{M_j^2}\right]-\frac{3}{2}m_j^4+2m_j^2M_j^2\right\} \tag{2.5}$$

where

$$\Delta\lambda=\frac{-1}{2v^2}\sum_j[\Sigma_j(M_h^2)-\Sigma_j(0)] \equiv\sum_j\frac{\mp g_jM_j^4}{128\pi^2v^4}f_j(M_h^2/M_j^2)\ . \tag{2.6}$$

The sums are over all particles j with g_j degrees of freedom and mass $m_j(\phi)$; we write $M_j\equiv m_j(v)$. The upper sign is for bosons, the lower for fermions. The standard model fields in the Landau gauge [1,5,25] are the Higgs bosons ($g_h=1$), the Goldstone bosons ($g_\chi=3$), the top quark ($g_t=12$), and the gauge bosons ($g_W=6, g_Z=3$), with tree-level masses

$$m_h^2=\lambda(3\phi^2-v^2)\ ,\quad m_\chi^2=\lambda(\phi^2-v^2)\ ,$$
$$m_t=\frac{M_t\phi}{v}\ ,\quad m_W=\frac{g\phi}{2}\ ,\quad m_Z=\frac{G\phi}{2}\ , \tag{2.7}$$

where $G^2=g^2+g'^2$.

In Appendix A we give the running functions $f_j(r)$ defined in Eq. (2.6). Note the Goldstone bosons, massless in Landau gauge for $\bar{\phi}=v$, contribute a logarithmic infinity to $\Sigma(0)$ and thus to $\Delta\lambda$, which exactly cancels the infinity in the $\ln[m_\chi^2/M_\chi^2]$ term.

The T-dependent part of the effective potential is [6–8,22,23]

$$V_T=g_j\frac{T^4}{2\pi^2}I_\pm(m_j/T)\ ,$$
$$I_\pm(y)\equiv\pm\int_0^\infty dx\,x^2\ln(1\mp e^{-\sqrt{x^2+y^2}})\ . \tag{2.8}$$

Series expansions of $I_\pm$ can be found in Appendix B. The ϕ^3 term arising from gauge boson loops is primarily responsible for the hump in the potential [1,5,26].

The Higgs and Goldstone masses can make imaginary contributions to V. For homogeneous field configurations, these represent the rate of decay to inhomogeneous states [21]. We speculate that for the critical bubble they are canceled (at least in large part) by derivative corrections [27]. The critical bubble has only one negative eigenmode (the "breathing" mode), whose contribution to the imaginary part of the action appears to be independent of the bubble radius R in the thin-wall limit, whereas the imaginary parts of V would contribute $\sim R^2$ to the action if uncanceled. It is also very suggestive that the region in which the integrand of Eq. (2.8) is complex ($x<|y|$, or $k<|m|$) arises from Fourier modes of ϕ with wavelengths larger than the bubble wall thickness [27,28]. We eliminate these modes by taking the real part of V_1 and changing the lower limit of integration in Eq. (2.8) to $\mathrm{Im}\{y\}$.

In the tadpole method [4,8,29], $V'(\bar{\phi})$ is calculated from tadpole graphs using Feynman rules in the shifted theory $\phi=\bar{\phi}+\phi'$, dropping linear terms in ϕ' which are canceled in the Legendre transform relating $W[J]$ and $\Gamma[\bar{\phi}]$ [Eq. (2.1)] [22,30]. The one-loop diagrams are shown in Fig. 1(a), giving (with $\tilde{m}=m$ for now)

$$V'=(\lambda+\Delta\lambda)\bar{\phi}(\bar{\phi}^2-v^2) + \sum_j\frac{\pm g_j}{32\pi^2}\frac{dm_j^2}{d\bar{\phi}}\left\{\tilde{m}_j^2\left[\ln\left[\frac{\tilde{m}_j^2}{M_j^2}\right]-1\right]+M_j^2\right\} + \sum_j\frac{g_jT^2}{24}\frac{dm_j^2}{d\bar{\phi}}F_\pm\left[\frac{\tilde{m}}{T}\right]\ , \tag{2.9}$$

where $F_\pm(y)\equiv 6I'_\pm(y)/(\pi^2 y)$.

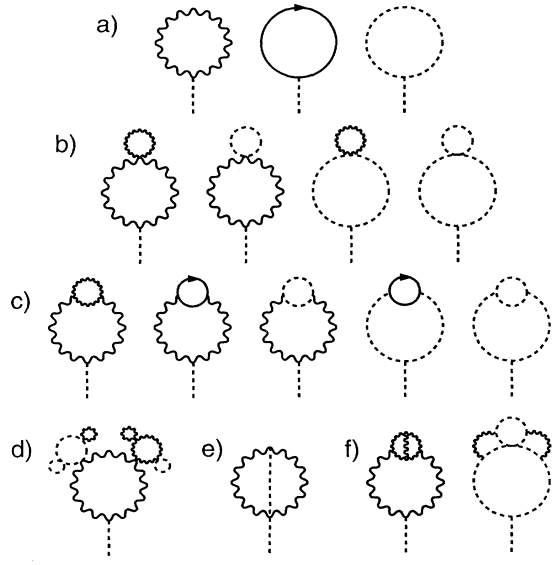

FIG. 1. Loop diagrams for V.

III. HIGHER-ORDER CORRECTIONS

Beyond one loop, the most important diagrams are daisies and superdaisies, as well as one other, the "lollipop" [Fig. 1(e)].

Consider the W tadpole [first diagram of Fig. 1(a)], which contributes $\sim(gT^2\mathcal{M})$ to V', where $\mathcal{M}\sim g\bar{\phi}$. "Daisies" [6] [Figs. 1(b) and 1(c)] are the diagrams with loops on the main W loop; those in Fig. 1(b) contribute $\sim(gT^2\mathcal{M})(g^2T^2/\mathcal{M}^2)^n(g^2T/\mathcal{M})$. If we ignore powers of $T/\bar{\phi}$, daisies are $O(g^3)$. "Superdaisies" [Fig. 1(d)] contribute $\sim(gT^2\mathcal{M})(g^2T^2/\mathcal{M}^2)^n(g^2T/\mathcal{M})^2$, and are $O(g^4)$ corrections. While many other diagrams exist which cannot be classified as daisies or superdaisies [Figs. 1(e) and 1(f)], only the "lollipop" [Fig. 1(e)] is $O(g^4)$. In the region of interest $(g^2T^2/\mathcal{M}^2)\approx 1$ and $(g^2T/\mathcal{M})<1$ [7], so we make a consistent approximation by considering superdaisy diagrams and the lollipop. In the Higgs sector the same categorization holds by replacing $g^2\to\lambda$.

We emphasize that the convergence properties of the loop expansion depend on the choice of $\bar{\phi}$ as well as T. For a given temperature T, the expansion may fail $[(g^2T/\mathcal{M})\geq 1]$ at some particular values of $\bar{\phi}$ due to uncontrolled IR divergences, while remaining good at other values of $\bar{\phi}$. A complete $O(g^4)$ calculation allows us to explore larger values of $T/\bar{\phi}$, while a partial calculation serves as an indicator of the reliability of our expansion.

Progress towards our goal is achieved by modifying the propagators D, as in Fig. 2. The largest $O(g^3)$ corrections are mass renormalizations, and are incorporated by replacing $\bar{m}$ in Eq. (2.9) with plasma masses [12]. Working to $O(g^4)$ requires a self-consistent solution of the mass gap equations. These are not the whole story, however, since we calculated the plasma masses at vanishing external momenta. Wave-function renormalization and the momentum dependence of the plasma masses must also be included. We plan to address these nonstatic corrections in a future publication, but make all effective potential calculations in this paper with self-energies evaluated at $\omega_n=0$ and three-momenta $\mathbf{k}=0$.

To put the various corrections in perspective, we estimate their contributions to the effective potential terms D, E, and λ_T, as well as to a "pseudolinear" term J, valid

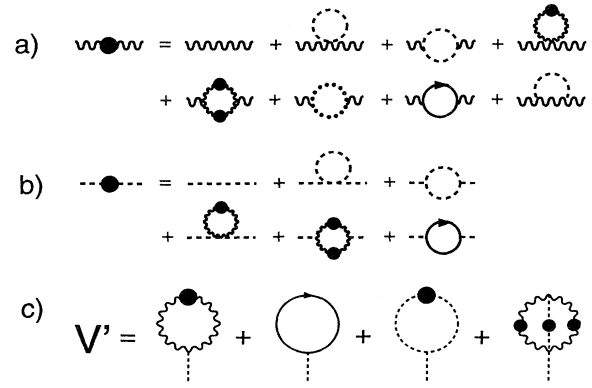

FIG. 2. Improved propagators.

TABLE I. Order of contributions to the potential.

	J	D	E	λ_T
One loop	0	g^2	g^3	g^4
Daisy $(\rho T^2<\bar{\phi}^2)$	g^3	g^4	g^7	g^6
Daisy $(\rho T^2>\bar{\phi}^2)$	0	g^3	g^3	g^{3a}
Superdaisy $(\rho T^2<\bar{\phi}^2)$	g^5	g^4	g^5	g^8
Superdaisy $(\rho T^2>\bar{\phi}^2)$	0	g^5	0	g^8
Lollipop	0	g^4	g^5	g^6
$\omega_n\neq 0(\rho T^2<\bar{\phi}^2)$	g^3	g^4	0	g^6
$\omega_n\neq 0(\rho T^2>\bar{\phi}^2)$	0	g^3	0	g^{3a}
$\omega_n=0,\mathbf{k}\neq 0$	0	g^4	g^5	g^6

[a]Suppressed by powers of ρ.

only when the tree mass is larger than the static plasma mass. Since daisy and superdaisy contributions are summed by mass renormalizations [valid at the tadpole level in the imaginary time formalism, where propagators go like $(k^2+m^2)^{-1}$], we schematically insert the relevant mass [see Eqs. (4.1), (4.3)] into Eq. (2.9), expand $F(\bar{m}/T)$ using Appendix B, and read off the J, D, E, and λ_T terms (see Table I). The terms involving ρ alone come from daisies, while those involving σ come from super daisies (and sub-leading terms in daisies).

The largest correction comes from daisies when $\rho T^2\gg\bar{\phi}^2$, because the introduction of an infrared cutoff eliminates the cubic term from the one-loop graph. The plasma mass of the W longitudinal mode corresponds to this case, while the Higgs plasma mass falls between the two extremes.

All of this is for static self-energies. We can use expressions, valid in unbroken theories, for the self-energy of gauge bosons [31] to estimate the contribution of nonzero frequency $\omega_n\neq 0$, or nonzero three-momentum $\mathbf{k}\neq 0$ propagator corrections. A typical correction is a self-energy term $g^2\rho\omega_n^2T^2/\mathbf{k}^2$. This gives a contribution

$$V'\sim g^2\bar{\phi}T\sum_n\int\frac{d^3\mathbf{k}}{(2\pi)^3}\left[\omega_n^2\left[1+\frac{g^2\rho T^2}{\mathbf{k}^2}\right]-\mathbf{k}^2-m^2\right]^{-1}$$

$$\sim g^2\bar{\phi}\int_m^T\frac{d^3\mathbf{k}}{\omega_0}F_{\omega_0}$$

$$\sim g^2T^2\bar{\phi}+\rho g^3\bar{\phi}T^3(\rho T^2+\bar{\phi}^2)^{-1/2}\,, \tag{3.1}$$

where $\omega_0^2=(\mathbf{k}^2+m^2)/(1+g^2T^2\rho/\mathbf{k}^2)$, and for purposes of power counting, F_x (defined in Appendix C) $\sim T/x$. For the table, we have assumed an expansion in m/T. In general, the nonstatic part of a tadpole is as important as the static part. However, in the unbroken theory [31] with $\omega_n=0$ (only $\omega_n=0$ contributes to E), the coefficient of $\mathbf{k}^2$ is down by $\sim 1/\pi^2$ relative to the coefficient of T^2, suggesting that $\bar{\phi}_+/T_c$ is not significantly altered by nonstatic terms. This contrasts with some recent claims [32].

IV. THE GAUGE SECTOR

To first approximation $\mathcal{M}=m_W=g\bar{\phi}/2$, so without propagator modification the loop expansion fails for $\bar{\phi}<T$, which is unacceptable. We solve the gap equation of Fig. 2(a) to obtain both electric and magnetic plasma

masses for the W. It is known [33] that, for $\bar{\phi}=0$, to leading order the magnetic plasma mass vanishes, so we write

$$\Pi_0^0=\rho_0 g^2T^2+\sigma_0 g^2 m_W T+O(g^4T^2)\ ,$$
$$\Pi_i^i=\sigma_i g^2 T m_W+O(g^4T^2)\ , \tag{4.1}$$

and solve

$$m_0=\sqrt{m_W^2+\Pi_0^0}\ ,\quad m_i=\sqrt{m_W^2+\Pi_i^i}\ . \tag{4.2}$$

The terms neglected [such as the distinction between m_i and m_0 on the right side of Eq. (4.1), or Higgs-sector contributions] are suppressed by powers of g,λ, or $(\mathcal{M}/T)$; see Appendix A. This procedure yields

$$m_0=\tfrac{1}{2}[\sigma_0 g^2T+\sqrt{(4\rho_0 g^2+\sigma_0^2 g^4)T^2+g^2\bar{\phi}^2}]\ , \tag{4.3}$$

$$m_i=\tfrac{1}{2}[\sigma_i g^2T+\sqrt{\sigma_i^2 g^4T^2+g^2\bar{\phi}^2}\ . \tag{4.4}$$

We calculate ρ_0, σ_0, and σ_i to one-loop for the standard model in Appendix A, but we will only use the result for $\sin\theta_W=\lambda=0$:

$$\rho_0=11/6\ ,\quad \sigma_0=-5/(4\pi)\ ,\quad \sigma=1/(6\pi) \tag{4.5}$$

We will treat the Z as a third W boson, but implicitly replace $g\to G$.

In Ref. [13] two of the authors used these masses in the vacuum-to-vacuum W loop, i.e., in Eq. (2.8), and found a linear term in V. At the tadpole level, this is equivalent to using both an improved propagator and an improved three point coupling [Fig. 3(a)]. For example, if $\tilde{m}^2$ is the plasma mass to $O(g^4)$, the vacuum-to-vacuum W loop generates a tadpole with improved Higgs-W-W coupling $ig_{\mu\nu}d\tilde{m}^2/d\bar{\phi}$ and improved inverse propagator $p^2+\tilde{m}^2$. This overcounts the "figure eight" tadpole as shown in Fig. 3(b), and is the source of the linear term (since the improved coupling does not vanish at $\bar{\phi}=0$). It is therefore important to make $\bar{\phi}$-dependent mass renormalizations at the tadpole level [16,34,41].

It has been suggested [32,35] that including the momentum dependence of the plasma masses eliminates the linear term. While it is true that the momentum dependence can be an important correction, any $\bar{\phi}$-dependent mass renormalization, whether or not it also depends on momentum, must be made at the tadpole (or mass, 3-point, etc.) level to avoid overcounting. We believe the linear term found by Shaposhnikov [14] arose from a similar overcounting.

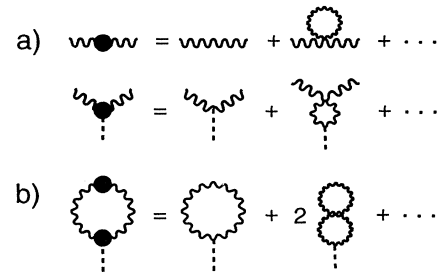

FIG. 3. Linear term tadpole, and overcounting.

Substituting the improved masses into the propagator in the W tadpole, counting all three W's, yields

$$V'=\frac{-3}{2}\frac{g^2\bar{\phi}}{2}T\sum_n\int\frac{d^3\mathbf{k}}{(2\pi)^3}\mathrm{Tr}\{P(1-\Pi P)^{-1}\} \tag{4.6}$$

where $-iP_\mu^\nu(k)$ is the Landau gauge tree-level propagator, and $\Pi_\mu^\nu=\mathrm{diag}(\Pi_0^0,\Pi_i^i,\Pi_i^i,\Pi_i^i)$. This gives

$$V'=\frac{3g^2\bar{\phi}}{4}T\sum_n\int\frac{d^3\mathbf{k}}{(2\pi)^3}\left[\frac{3}{k_i^2}-\frac{\mathbf{k}^2\delta}{k_i^2(k_n^2k_i^2+\mathbf{k}^2\delta)}\right]\ , \tag{4.7}$$

where $k_n^2\equiv\mathbf{k}^2+(2\pi nT)^2$, $k_i^2=k_n^2+m_i^2$, and $\delta\equiv\Pi_0^0-\Pi_i^i=m_0^2-m_i^2$. The first term in brackets exactly reproduces Eq. (2.9) with $\tilde{m}\to m_i$. The second term, up to renormalizable divergences, is dominated by $n=0$ and is approximately

$$\frac{3g^2\bar{\phi}}{4}\frac{T(m_i-m_0)}{4\pi}\ . \tag{4.8}$$

Insofar as $m_i\sim\bar{\phi}$ and $m_0\sim T$, this term reduces the cubic term in V by $\frac{1}{3}$, as expected [16]. In Appendix C we show there is an additional (relatively unimportant) correction:

$$\frac{3g^2\bar{\phi}}{4}\frac{3\delta}{64\pi^2}[\ln(T^2/M_W^2)+5.21]\ . \tag{4.9}$$

We next turn to the lollipop diagram [Fig. 1(e)], with propagators improved to $O(g^2)$. The contribution of internal $W^\pm$'s to V' is

$$V_l'=\frac{-g^3M_w}{2}T\sum_n\int\frac{d^3\mathbf{k}}{(2\pi)^3}T\sum_m\int\frac{d^3\mathbf{p}}{(2\pi)^3}\frac{1}{[(p_m-k_n)^2+m_h^2]}\mathrm{Tr}\{P(k)[1-\Pi P(k)]^{-1}P(p)[1-\Pi P(p)]^{-1}\}\ . \tag{4.10}$$

There is also a contribution due to the Z. Details of the computation are left to Appendix C, where the expression is evaluated for static self energies and $\delta=0,\infty$.

Finally, we remark on our gauge fixing. In R_ξ renormalizable gauges, the gauge–Goldstone-boson mixing can be eliminated only if one chooses a different gauge for every value of $\bar{\phi}$. Although the potential can be modified to account for this [36], it is unnecessary in the case of Landau gauge, where the mixing term vanishes due to $\partial_\mu A^\mu=0$.

V. THE HIGGS SECTOR

It is easy to include the effects of gauge bosons and fermion loops on the Higgs propagator, since the effective potential is the generating function of 1PI graphs at zero

external momentum. If V_G is the potential calculated from gauge bosons and fermions only, then the shifted Higgs boson mass $m_h^2 = V_G''$ and the Goldstone boson mass $m_\chi^2 = V_G'/\bar{\phi}$. We could solve the gap equation (to include superdaisies) as we did for the gauge sector, giving

$$m_h^2(\bar{\phi},T) = V_G''(\bar{\phi},T) + \frac{\lambda T^2}{4}\left[F_+\left[\frac{m_h}{T}\right] + F_+\left[\frac{m_\chi}{T}\right]\right] + \frac{\lambda^2\bar{\phi}^2 T}{4}\left[\frac{3}{m_h}F_+'\left[\frac{m_h}{T}\right]\frac{1}{m_\chi}F_+'\left[\frac{m_\chi}{T}\right]\right],$$

$$m_\chi^2(\bar{\phi},T) = V_G'(\bar{\phi},T)/\bar{\phi} + \frac{\lambda T^2}{12}\left[F_+\left[\frac{m_h}{T}\right] + 5F_+\left[\frac{m_\chi}{T}\right]\right] + \frac{\lambda^2\bar{\phi}^2 T^2}{3(m_h^2 - m_\chi^2)}\left[F_+\left[\frac{m_h}{T}\right] - F_+\left[\frac{m_\chi}{T}\right]\right]. \tag{5.1}$$

However, except for very heavy Higgs bosons these are well approximated by

$$m_h^2(\bar{\phi},T) = V_G''(\bar{\phi},T) + \frac{\lambda T^2}{2},$$

$$m_\chi^2(\bar{\phi},T) = V_G'(\bar{\phi},T)/\bar{\phi} + \frac{\lambda T^2}{2} \tag{5.2}$$

which corresponds to Fig. 2(b). These are the masses $\tilde{m}$ we use in Eq. (2.9). Thus, we have summed contributions to the Higgs boson mass due to gauge boson superdaisies, but only Higgs daisies.

Carrington [15], working to lowest order in g, essentially found Eq. (5.2) but with V_G'' and $V_G'/\bar{\phi}$ replaced by their values at the origin. Thus at all interesting temperatures the scalar masses appeared real. Our calculation reintroduces imaginary masses; see the discussion following Eq. (2.8). Some bumpiness results in our plots where m_h and m_χ pass through zero.

VI. IMPROVING THE STANDARD MODEL EFFECTIVE POTENTIAL

We first calculate the "one-loop" effective potential. Then we omit the Higgs sector and improve the gauge sector as described in Eq. (4.7) and the subsequent paragraph to get V_G. The Higgs sector is then added back in using Eq. (5.2) in Eq. (2.9), adding the lollipop from Appendix C, and integrating to get the "superdaisy" potential, as in Fig. 2(c).

For comparison we also show a "daisy" potential, which differs only in setting $\sigma_0 = \sigma_i = 0$ in Eq. (4.3) and Eq. (4.4) and omitting the lollipop. A good "estimate" is obtained by calculating the one-loop potential with $g_W = 4$, $g_Z = 2$, and $m_h = m_\chi = 0$.

Figure 4 shows these potentials for various values of the Higgs and top masses (in GeV), including one set matching Carrington's plots [15]. Each potential is shown at its critical temperature T_1 (i.e., when two vacua

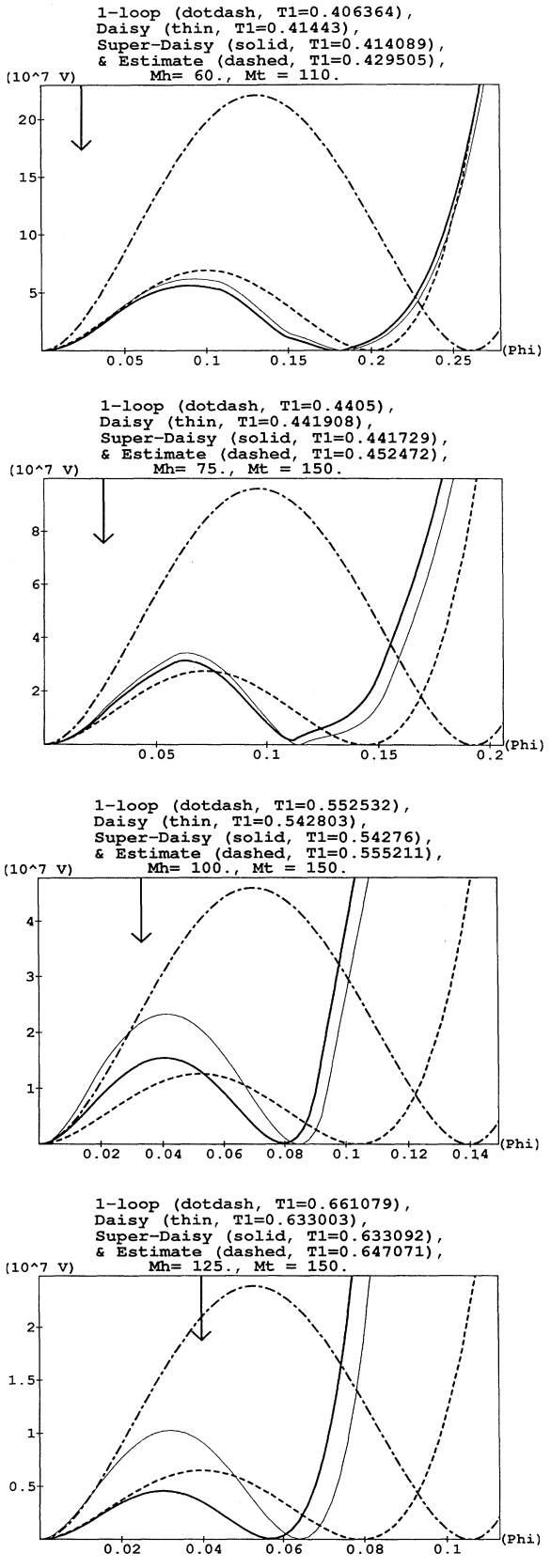

FIG. 4. One-loop, daisy, superdaisy and estimate potentials.

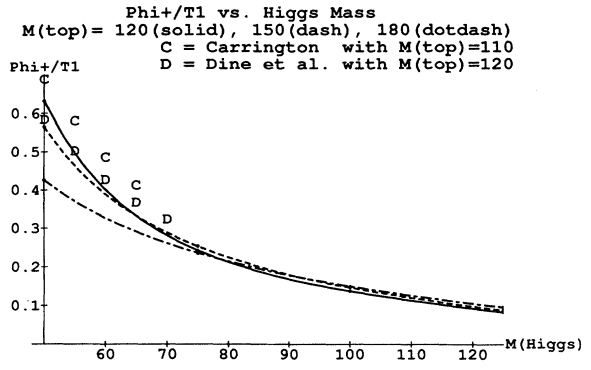

FIG. 5. ϕ_+/T_1 vs M_h.

are degenerate). V, $\bar{\phi}$, and T are given in units where $v=1$.

For $\bar{\phi} \gg 2T$ the plasma mass corrections are small, and the one-loop potential is adequate. The perturbative expansion is still out of control for $g^2T/m_i > 4\pi$ (where the numerical factor is something of a guess), or roughly $\bar{\phi} < 0.06T$ (marked by an arrow on the plots), so even the "superdaisy" potential is not to be trusted far to the left of the arrow. This is about a factor of 2 closer to the origin than the corresponding cutoff for the "daisy" potential, $\bar{\phi} < 0.10T$ [15]. Indeed we see that for $M_h > 75$ GeV the "daisy" and "superdaisy" potentials differ significantly.

We plot $\phi_+(T_1)/T_1$ [which closely approximates $\phi_+(T_b)/T_b$] vs M_h for several values of M_t in Fig. 5. For comparison we show values from both Carrington [15], Fig. 14 (with $M_t = 110$ GeV), and Dine *et al.*, Fig. 5 ($M_t = 120$ GeV); in the latter case we converted their results at T_b (which they call T_t for "tunneling") using the quartic potential relation

$$\frac{\phi_+(T_1)}{T_1} = \frac{\phi_+(T_b)}{T_b}\left[\frac{4}{3+\sqrt{1+8\epsilon_b}}\right],$$
$$\epsilon_b \equiv \frac{T_1^2 - T_b^2}{T_1^2 - T_2^2} \tag{6.1}$$

and took ϵ_b from their Fig. 6. For a light Higgs boson, where $O(g^4)$ corrections are small (see Fig. 4), all the results agree closely. As the Higgs mass increases, higher-order corrections appear to lower $\phi_+(T_1)/T_1$. We note the top mass is nearly irrelevant for heavier Higgs bosons. Since $\phi_+(T_1)/T_1 \ll 1.4$ for all experimentally-allowed Higgs and top masses, we see the EWPT remains too weakly first order to drive baryogenesis.

VII. SADDLE POINTS AND THE EFFECTIVE ACTION

While the effective potential suffices to determine the order of the transition, the full action Γ [see Eq. (2.2)] is needed to determine the dynamical properties of the system, such as the rates for bubble nucleation or sphaleron fluctuations. For extremal configurations such as critical bubbles, $J=0$ in Eq. (2.1) and $\Gamma[\bar{\phi}] = W[0]$ is gauge invariant [37], so derivative terms must cancel out the gauge dependence of V.

We can use Chan's derivative expansion [18] to estimate the size of derivative corrections. Since the finite temperature Green's functions $G(x,y)$ satisfy the same equations as the zero temperature ones, but with periodic boundary conditions, we may formally express $G(x,y)$, in the Landau gauge, as

$$G(x,y) = T\sum_n \int \frac{d^3\mathbf{p}}{(2\pi)^3} e^{ip\cdot y}[-\partial_x^2 + U(x)]^{-1} e^{-ip\cdot x}, \tag{7.1}$$

where $U(x)$ is the mass of the field in question, including $\bar{\phi}$-independent plasma corrections. Following Chan's technique, we write $G(x,x)$ as an explicit expansion in even powers of derivatives:

$$G(x,x) = T\sum_n \int \frac{d^3\mathbf{k}}{(2\pi)^3}\left[k^2 + U\left[x + i\left[\frac{\partial}{\partial k}\right]\right]\right]^{-1}$$
$$= T\sum_n \int \frac{d^3\mathbf{k}}{(2\pi)^3}[k^2+U(x)]^{-1}\sum_m^{\infty}\left[-\sum_q^{\infty}\frac{1}{q!}[\partial_{j_1}\cdots\partial_{j_q}U(x)]\left[i\frac{\partial}{\partial k_{j_1}}\cdots i\frac{\partial}{\partial k_{j_q}}\right][p^2+U(x)]^{-1}\right]^m, \tag{7.2}$$

The contribution to the spatial part of the kinetic energy arises from the $m=1, q=2$ and $m=2, q=1$ terms in the above sum. Taking only the dominant $n=0$ part of the frequency sum gives

$$\mathcal{L}_{\text{eff}} \ni -\tfrac{1}{2}\int \delta U(x) G(x,x)$$
$$= \frac{-g_j T}{384\pi} U^{-3/2}(U')^2(\partial_i\bar{\phi})^2$$
$$= \frac{-1}{64\pi}\frac{g^2 T}{(g\bar{\phi}/2)}(\partial_i\bar{\phi})^2 \tag{7.3}$$

where $U = m_j^2(\bar{\phi})$, and ∂_i is a spatial derivative. We have inserted values for the tree-level W mass in the second expression, corresponding to the $\mathbf{p}^2$ term of the penultimate diagram in Fig. 2(b).

The form is as expected by naive power counting of a one-loop graph with two external legs, both carrying nonzero momentum. Since this $O(g)$ contribution is nu-

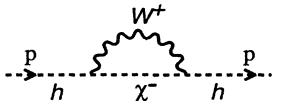

FIG. 6. Momentum-dependent Higgs self-energy at $O(g^2)$.

merically small, one might think derivative corrections are unimportant. That this may *not* be the case is indicated by the calculation of the $O(g^2)$ graph in Fig. 6.

This graph arises in the derivative expansion from a shifting of G^{-1} due to mixing which we previously ignored. Its contribution (setting $s_w=0$) to the real part of the Higgs self-energy, with real external four-momentum p, is

$$\Pi(p_0,\mathbf{p})=3g^2T\sum_n\int\frac{d^3\mathbf{k}}{(2\pi)^3}\frac{p^2-(p\cdot k)^2/k^2}{(k^2+m_W^2)[(p+k)^2+m_\chi^2]}$$
$$=3g^2\left\{\left[\frac{5}{8}p^2+\frac{m_\chi^2-m_W^2}{8}\right]L\left[\frac{m_W^2-m_\chi^2-p^2}{2};p_0,\mathbf{p}\right]+\left[\frac{m_\chi^2}{8}-\frac{3}{8}p^2\right]L\left[\frac{-p^2-m_\chi^2}{2};p_0,\mathbf{p}\right]\right.$$
$$-\frac{(p^2-m_\chi^2)^2}{8m_W^2}L\left[\frac{p^2-m_\chi^2}{2};p_0,\mathbf{p}\right]+\left[\frac{(p^2-m_\chi^2+m_W^2)^2}{8m_W^2}-\frac{1}{2}p^2\right]L\left[\frac{p^2+m_W^2-m_\chi^2}{2},p_0,\mathbf{p}\right]$$
$$+\frac{p^4+m_\chi^2(m_\chi^2-m_W^2)+p^2(3m_W^2-2m_\chi^2)}{16(p^2+m_\chi^2-m_W^2/2)}\left[L\left[\frac{m_W^2}{2}-p^2-m_\chi^2;p_0,\mathbf{p}\right]\right.$$
$$\left.\left.+L\left[0;-p_0,\mathbf{p}\right]\right]\right\}+O\left[\frac{m^2}{T^2}\right] \tag{7.4}$$

in which

$$L(m^2;p_0,\mathbf{p})=\int_0^\infty\frac{dk}{2\mathbf{p}(2\pi)^2}\left[F_k\ln\left|\frac{k(\mathbf{p}-p_0)-m^2}{k(\mathbf{p}+p_0)+m^2}\right|+F_{-k}\ln\left|\frac{k(\mathbf{p}-p_0)+m^2}{k(\mathbf{p}+p_0)-m^2}\right|\right] \tag{7.5}$$

and $\mathbf{p}$ is the magnitude of the external three-momentum.

The integral has been computed previously [31], to $O(T^{-2})$. After a minor algebraic correction, it gives

$$L(m^2;p_0,\mathbf{p})=\frac{T}{8\mathbf{p}}\theta(-p^2)\mathrm{sgn}(-m^2)+\frac{m^2}{4\pi^2p^2}\left[\frac{p_0}{2\mathbf{p}}\ln\left|\frac{p_0+\mathbf{p}}{p_0-\mathbf{p}}\right|+\gamma_{\text{Euler}}-1+\frac{1}{2}\ln\frac{M_W^2}{4\pi^2T^2}\right] \tag{7.6}$$

where M_W is our subtraction point, and $\mathrm{sgn}(0)=0$. The analytic behavior of this diagram [note the strange $T/\mathbf{p}$ behavior of $L(m^2;p_0,\mathbf{p})$] is sensitive to the scheme one uses to continue from imaginary to real external momentum. Our continuation prescription is consistent with previous work [31,38], but there are other methods [39]. The $p_0=0$, $\mathbf{p}\neq0$ behavior, which characterizes saddle point solutions, may be altered if our prescription turns out to be incorrect.

VIII. CONCLUSION

Much recent work on the EWPT [13–16,32] has concentrated on improving the calculation of V. We now believe there is no linear term, and that the propagator improvement performed in Ref. [15] and estimated in Ref. [16] is essentially correct for the gauge sector to $O(g^3)$. The main result of these corrections is to screen the longitudinal mode, decreasing the cubic term E by a factor of $\frac{1}{3}$ and making the transition more weakly first order.

In this paper we have included higher-order corrections not previously considered, specifically those from subleading parts of daisy graphs, gauge superdaisies, gauge superdaisies in the Higgs sector, and the "lollipop" diagram. We estimated the effect on the effective potential of using momentum-dependent self-energies, and computed the $O(g^2)$ derivative corrections to the effective action. The results of our effective potential computations are similar to those of [15,16] for a light Higgs ($M_h\leq75$ GeV), but show an even further weakening of the transition for a heavier Higgs (75 GeV $<M_h<$ 125 GeV). Above 125 GeV our expansion becomes less reliable.

Evans [32] has criticized all recent calculations of the electroweak effective potential on the grounds that propagator resummations have been performed at zero external momentum, rather than on shell. We find that although this approximation does lead to errors (as pointed out in our earlier paper [13]), they are unlikely to lead to any qualitative changes in the behavior of the potential.

Derivative corrections to the effective action may be important, however. For example, if the diagram in Fig. 6 is indicative, they could significantly alter bounce solutions when typical spatial frequencies are less than about $T/8$. Estimates of bubble wall thicknesses are often tens of T^{-1} [16,40]. Similar corrections to the gauge boson effective action could distort the sphaleron solution.

To summarize, a computation of V in any finite-loop approximation is subject to uncontrolled infrared corrections for $\bar{\phi}<T$. When plasma masses are included in both the gauge and Higgs sectors, the improved potential is reliable for $\bar{\phi}>gT/10$. We have computed V for the standard model, and compared the results to previous estimates. If current estimates of sphaleron energies are re-

liable, the standard model (even with augmented *CP* violation) is still inadequate to generate the baryon asymmetry.

Note added in proof. Subsequent work [41] has analyzed the standard model effective potential including momentum-dependent plasma masses, by explicitly calculating all the relevant diagrams with overlapping momenta. The logarithmic corrections which arise appear to be significant.

ACKNOWLEDGMENTS

The authors would like to thank Greg Anderson, Peter Arnold, Meg Carrington, Michael Dine, Thomas Gould, Lawrence Hall, Clarence Lee, Andrei Linde, Ann Nelson, Stamatis Vokos, Erick Weinberg, and Mark Wise for numerous discussions. We thank J. R. Espinosa and M. Quiros [42] for pointing out misprints in an earlier version's Eqs. (10.4) and (10.5). D.E.B. acknowledges support from the U.S. Department of Energy under Contract No. DE-FG03-92-ER40701, and thanks the Stanford Linear Accelerator Center for its hospitality during part of this work. S.D.H. acknowledges support from the National Science Foundation under Grant No. NSF-PHY-87-14654, the state of Texas under Grant No. TNRLC-RGFY106, and from the Harvard Society of Fellows. C.G.B. acknowledges support from the U.S. Department of Energy under Contract. No. DEFG-02-90ER40560, as well as the National Science Foundation under Grant No. NSF-PHY-91-23780.

APPENDIX A: STANDARD MODEL f_j's and Π's

The functions $f_j(r)$ defined in Eq. (2.6) are (to one-loop)

$$f_h(1)=18(\pi/\sqrt{3}-2)\ ,$$

$$f_\chi(r)=\frac{8\lambda^2 v^4}{M_\chi^4}[\ln(r)+i\pi-2]\ ,$$

$$f_t(r)=\frac{4(4-r)^2}{\sqrt{4r-r^2}}\arctan\left[\frac{r}{\sqrt{4r-r^2}}\right]-16+2r\ ,$$

$$f_W(r)=f_Z(r)$$
$$=\frac{4}{3}\left[\frac{4-r}{r}\right]^{1/2}(r^2-4r+12)\arctan\left[\frac{r}{\sqrt{4r-r^2}}\right]$$
$$+\frac{4(1-r)^3}{3r}\ln(1-r)-\frac{44}{3}+\frac{2r^2}{3}[\ln(r)-i\pi]\ . \tag{A1}$$

Note the imaginary part of f_χ (representing the amplitude for a Higgs boson to decay to Goldstone bosons in the ungauged theory) is exactly canceled by a term in $f_{W,Z}$. For large r, the leading results for the top and the gauge bosons [corresponding to taking $\Sigma(M_h^2)-\Sigma(0)=M_h^2\Sigma'(0)$] are

$$f_t(r)\approx -10r/3\ ,\quad f_W(r)=f_Z(r)\approx -10r/3\ . \tag{A2}$$

The electric and magnetic plasma masses for the $W^\pm$ from Fig. 2(a) are

$$\Pi_0^0(W^\pm)=\frac{g^2T^2}{3}\left[2+\frac{1}{2}+\frac{12}{4}\right]-\frac{g^2T}{2\pi}\left[m_W+c_W^2m_Z+s_W^2m_\gamma+\frac{m_h+3m_\chi}{8}\right]$$
$$-\frac{g^4\phi^2T}{16\pi}\left[\frac{1}{m_h+m_W}+\frac{s_W^2}{m_\chi+m_\gamma}+\frac{s_W^4/c_W^2}{m_\chi+m_Z}\right]\ ,$$

$$\Pi_i^i(W^\pm)=\frac{g^2T}{\pi}\left[\frac{-7}{12}(m_W+c_W^2m_Z+s_W^2m_\gamma)+c_W^2\frac{m_Z^3-m_W^3}{m_Z^2-m_W^2}+s_W^2\frac{m_W^3-m_\gamma^3}{m_W^2-m_\gamma^2}-\frac{m_h+m_\chi}{16}+\frac{1}{12}\frac{m_h^3-m_\chi^3}{m_h^2-m_\chi^2}\right]$$
$$-\frac{g^4\phi^2T}{24\pi}\left[\frac{1}{m_h+m_W}+\frac{s_W^2}{m_\chi+m_\gamma}+\frac{s_W^4/c_W^2}{m_\chi+m_Z}\right]\ . \tag{A3}$$

The three numbers in brackets in the first term of Π_0^0 reflect contributions from the gauge sector, the Higgs sector, and 12 fermionic isospin doublets, respectively.

The analogous formulas for the Z^0 are

$$\Pi_0^0(Z^0)=\frac{g^2T^2}{3}\left[2c_W^2+\frac{1}{2}\frac{1-2s_W^2c_W^2}{c_W^2}+\frac{12}{4}\frac{1-2s_W^2+8s_W^4/3}{c_W^2}\right]$$
$$-\frac{g^2T}{2\pi}\left[2c_W^2m_W+\frac{m_h+(3-8s_W^2c_W^2)m_\chi}{8}\right]-\frac{g^4\phi^2T}{16\pi}\left[\frac{1/c_W^4}{m_h+m_Z}+\frac{2s_W^4/c_W^2}{m_\chi+m_W}\right]\ ,$$

$$\Pi_i^i(Z^0)=\frac{g^2T}{\pi}\left[\frac{c_W^2}{3}m_W-\frac{m_h+m_\chi}{16c_W^2}+\frac{1}{12c_W^2}\frac{m_h^3-m_\chi^3}{m_h^2-m_\chi^2}\right]-\frac{g^4\phi^2T}{24\pi}\left[\frac{1/c_W^4}{m_h+m_Z}+\frac{2s_W^4/c_W^2}{m_\chi+m_W}\right] \tag{A4}$$

and for the photon

$$\Pi_0^0(\gamma)=\frac{e^2T^2}{3}[2+1+8]-\frac{e^2T}{2\pi}[2m_W+m_\chi]-\frac{e^2g^2\phi^2T}{8\pi(m_\chi+m_W)}\ ,$$

$$\Pi_i^i(\gamma)=\frac{e^2T}{\pi}\left[\frac{1}{3}m_W\right]-\frac{e^2g^2\phi^2T}{12\pi(m_\chi+m_W)}\ . \tag{A5}$$

We do not distinguish m_i, m_0, and m_W in the Π's; the resulting error in the gap equations Eq. (4.1) is $O(g^4T^2)$. To further simplify things, we take $s_W\to 0$ (with g constant), introducing an error $O(e)=O(gs_W)$; and we set $m_h=m_\chi=0$, since these masses (V'' and $V'/\bar{\phi}$, respectively) vanish near the phase transition. Then the $W^\pm$ and Z^0 self-energies both become

$$\Pi_0^0\approx\frac{11g^2T^2}{6}-\frac{5g^2T}{4\pi}m_W\ ,\quad \Pi_i^i\approx\frac{g^2T}{6\pi}m_W \tag{A6}$$

which gives Eq. (4.5).

APPENDIX B: NUMERICAL APPROXIMATIONS FOR $I_\pm$

The following approximations [5,6,43,44] to $I_\pm$ [see Eq. (2.8) and the following paragraph] are accurate to 10^{-4}:

$$I_+(y<1)\approx\frac{-\pi^4}{45}+\frac{\pi^2}{12}y^2-\frac{\pi}{6}y^3-\frac{y^4}{32}(\ln y^2-5.4076)+0.00031y^6\ , \tag{B1}$$

$$I_-(y<1)\approx\frac{-7\pi^4}{360}+\frac{\pi^2}{24}y^2+\frac{y^4}{32}(\ln y^2-2.6350)-0.00214y^6\ , \tag{B2}$$

$$I_+(i(y<1))\approx\frac{-\pi^4}{45}-\frac{\pi^2}{12}y^2+y^3\left[\frac{4}{9}-\frac{1}{3}\ln(2y)\right]-\frac{y^4}{32}(\ln y^2-5.4076)+\frac{y^5}{180}-0.00029y^6\ , \tag{B3}$$

$$I_+(y>1)=-\sum_{n=1}^{\infty}\frac{y^2K_2(ny)}{n^2}\ , \tag{B4}$$

$$I_-(y>1)=\sum_{n=1}^{\infty}(-1)^n\frac{y^2K_2(ny)}{n^2}\ , \tag{B5}$$

$$\begin{aligned}I_+(i(y>1))=&\sum_{n=1}^{[8/y]}\left\{\frac{y^3}{3n}-\frac{\pi y^2}{2n^2}[\mathcal{H}_2(ny)-Y_2(ny)]\right\}\ ,\\&+\frac{y}{\pi}\sum_{j=0}^{4}\left\{\left[\zeta(2j+3)-\sum_{n=1}^{[8/y]}n^{-(2j+3)}\right]\left[\frac{-4}{y^2}\right]^j\Gamma\left[j+\frac{3}{2}\right]\Gamma\left[j-\frac{1}{2}\right]\right\}\end{aligned} \tag{B6}$$

where K and Y are Bessel functions, $\mathcal{H}$ is the Struve function, ζ is the Riemann zeta function, $[x]$ is the greatest integer less than or equal to x, and infinite sums are terminated when the desired accuracy is achieved.

We note that the $\phi^4\ln\phi^2$ term which come from $I_\pm(g\phi/T)$ and those which come from the $T=0$ potential cancel.

APPENDIX C: GAUGE TADPOLE AND LOLLIPOP

We may rewrite Eq. (4.7) a

$$V'=\frac{3g^2\bar{\phi}}{4}T\sum_n\int\frac{d^3\mathbf{k}}{(2\pi)^3}\left[\frac{2}{k_i^2}+\frac{k_n^2}{k_n^2k_i^2+\mathbf{k}^2\delta}\right] \tag{C1}$$

and evaluate the sum with the usual contour integral trick. The second term then becomes

$$\frac{3g^2\bar{\phi}}{4}\int\frac{d^3\mathbf{k}}{(2\pi)^3}\left[\frac{k_++k_-+\frac{m_i^2}{\Delta}(k_--k_+)}{4\sqrt{k^4+m_0^2k^2}}+\frac{m_i^2}{2\Delta}\left[\frac{F_{k_+}}{k_+}-\frac{F_{k_-}}{k_-}\right]+\frac{F_{k_+}}{2k_+}+\frac{F_{k_-}}{k_-}\right]\ , \tag{C2}$$

where $\Delta=\sqrt{m_i^4-4\delta k^2}$, $k_\pm=\sqrt{k^2+m_i^2/2\pm\Delta/2}$, and $F_x=[e^{x/T}-1]^{-1}$.

After renormalization, Eq. (C2) is well approximated by

$$\frac{m_i^2}{16\pi^2}\left[\ln\frac{m_i^2}{M_W^2}-0.39\right]+\frac{3\delta}{64\pi^2}\left[\ln\frac{T^2}{M_W^2}+5.21\right]+\frac{T^2}{12}F\left[\frac{m_i}{T}\right]+\frac{T}{4\pi}(m_i-m_0)\ . \tag{C3}$$

Note that although the $k_\pm$ can be complex, the final answer is real.

The lollipop, Eq. (4.10), has been evaluated elsewhere in unitary gauge [45] with unimproved propagators. In Landau gauge, it is somewhat more complicated. For static self-energies,

$$\mathrm{Tr}\{P(k)[1-\Pi P(k)]^{-1}P(p)[1-\Pi P(p)]^{-1}\}=\frac{1}{k_i^2p_i^2}\left[2+\frac{(k_n\cdot p_m)^2}{k_n^2p_m^2}-X\delta\right], \tag{C4}$$

where $p_i^2=p_m^2+m_i^2$ and

$$X=(k_n\cdot p_m)^2\frac{k_\delta^4\mathbf{p}^2+p_\delta\mathbf{k}^2-\mathbf{k}^2\mathbf{p}^2\delta}{k_n^2k_i^2k_\delta^4p_n^2p_i^2p_\delta^4}+[\mathbf{k}^2\mathbf{p}^2-(\mathbf{k}\cdot\mathbf{p})^2]\frac{k_i^2+p_i^2+\delta}{k_i^2p_i^2k_\delta^4p_\delta^4} \tag{C5}$$

in which $k_\delta^4=k_n^2k_i^2+\mathbf{k}^2\delta$.

The frequency sums can be evaluated by using the contour trick: For $f(p)=g(p;k)/[(p-k)^2-m^2]$, $p_0=2\pi inT$, and $g(p,k)$ nonsingular at the explicit pole, the contribution from the pole is

$$T\sum_m\int\frac{d^3\mathbf{p}}{(2\pi)^3}f(p)=-\int\frac{d^4p}{(2\pi)^3}\mathrm{sgn}(p_0)\delta(p^2-m^2)F_{p_0+k_0}g(p+k;k)\ . \tag{C6}$$

For $k_0=2\pi imT$ (i.e., an internal momentum), $F_{p_0+k_0}=F_{p_0}$. This formula should be applied to each pole in Eq. (C4).

Temperature-dependent infinities are canceled by graphs analogous to the lollipop, but with insertions of zero-temperature counterterms. The finite part of Eq. (4.10) is, for $\delta=0$,

$$V_l'=\frac{g^3M_W}{2}\left[\left[3/2-\frac{m_h^2(m_i^2+m_h^2)}{2m_i^4}\right]A\left[\frac{m^2}{2}\right]+\frac{(m_i^2-m_h^2)^2}{2m_i^4}A\left[\frac{m_h^2-m_i^2}{2}\right]\right.$$
$$\left.-\left[\frac{3}{4}+\frac{m_h^4}{4m_i^4}\right]A\left[\frac{m_h^2+m_i^2}{2}\right]+\left[\frac{m_h^2}{2m_i^2}-\frac{m_h^4}{8m_i^4}-\frac{3}{2}\right]A\left[\frac{m_h^2-2m_i^2}{2}\right]\right] \tag{C7}$$

where

$$A(m)=\int_0^\infty\frac{dk\,dp}{(2\pi)^4}F_{k_0}F_{p_0}\ln\left|\frac{m^2-2pk}{m^2+2pk}\right| \tag{C8}$$

$$\approx 3.11\times10^{-5}T^2\left[\ln\frac{m^2}{T^2}-1\right]. \tag{C9}$$

For $\delta\to\infty$,

$$V_l'=\frac{g^3M_W}{2}\left[B\left[m_h^2,\frac{m_h^2}{2}\right]-\frac{1}{2}B\left[m_i^2,\frac{m_h^2-2m_i^2}{2}\right]\right] \tag{C10}$$

where

$$B(m^2,M^2)=\int_0^\infty\frac{dk\,dp}{(2\pi)^4}F_aF_b\frac{kp}{2ab}\left\{\frac{4M^2}{kp}+\left[1+\frac{(M^2-ab)^2}{k^2p^2}\right]\ln\left|\frac{kp+M^2-ab}{kp-M^2+ab}\right|\right.$$
$$\left.+\left[1+\frac{(M^2+ab)^2}{k^2p^2}\right]\ln\left|\frac{kp+M^2+ab}{kp-M^2-ab}\right|\right\} \tag{C11}$$

and $a^2=k^2+m_i^2$, $b^2=p^2+m^2$. A numerical approximation to Eq. (C10) is

$$V_l'\approx\frac{g^3M_W}{2}0.002T^2\left[\frac{m_h}{m_i}e^{-0.9(m_h+m_i)/T}-\frac{m_h^2-2m_i^2}{2m_i^2}e^{-1.8m_i/T}\right]. \tag{C12}$$

We used $\delta=\infty$ in all plots in this paper.

[1] M. Dine, P. Huet, R. Singleton, Jr., and L. Susskind, Phys. Lett. B **257**, 351 (1991); Nucl. Phys. **B375**, 625 (1992).

[2] M. E. Shaposhnikov, Nucl. Phys. **B287**, 757 (1987); A. I. Bochkarev and M. E. Shaposhnikov, Mod. Phys. Lett. A **417** (1987); L. McLerran, M. Shaposhnikov, N. Turok, and M. Voloshin, Phys. Lett. B **256**, 451 (1991); A. Cohen, D. Kaplan, and A. Nelson, *ibid.* **245**, 561 (1990); Nucl. Phys. **B349**, 727 (1991); **B373**, 453 (1992).

[3] A. D. Sakharov, Pis'ma Zh. Eksp. Teor. Fiz. **5**, 32 (1967) [JETP Lett. **5**, 24 (1967)].
[4] D. Kirzhnits and A. Linde, Ann. Phys. (N.Y.) **101**, 195 (1976).
[5] G. W. Anderson and L. J. Hall, Phys. Rev. D **45**, 2685 (1992).
[6] L. Dolan and R. Jackiw, Phys. Rev. D **9**, 3320 (1974).
[7] S. Weinberg, Phys. Rev. D **9**, 3357 (1974).
[8] D. Kirzhnits and A. Linde, Zh. Eksp. Teor. Fiz. **67**, 1263 (1974) [Sov. Phys. JETP **40**, 628 (1975)].
[9] A. D. Linde, Nucl. Phys. **B216**, 421 (1983).
[10] ALEPH Collaboration, D. Decamp *et al.*, Phys. Rep. **216**, 253 (1992); Report No. CERN-PPE/91-19, 1991 (unpublished).
[11] S. Weinberg, in *Understanding the Fundamental Constituents of Matter,* edited by Antonio Zichichi (Plenum, New York, 1978).
[12] A. Linde, Phys. Lett. **96B**, 289 (1980); K. Takahashi, Z. Phys. C **26**, 601 (1985); P. Fendley, Phys. Lett. B **196**, 175 (1987); J. Kapusta, *Finite Temperature Field Theory* (Cambridge University Press, Cambridge, England, 1989).
[13] D. E. Brahm and S. D. H. Hsu, Report No. CALT-68-1705/HUTP-91-A063 (unpublished).
[14] M. E. Shaposhnikov, Phys. Lett. B **277**, 324 (1992).
[15] M. E. Carrington, Phys. Rev. D **45**, 2933 (1992).
[16] M. Dine, R. G. Leigh, P. Huet, A. Linde, and D. Linde, Phys. Lett. B **283**, 319 (1992); Phys. Rev. D **46**, 550 (1992).
[17] P. Arnold (private communication).
[18] L.-H. Chan, Phys. Rev. Lett. **54**, 1222 (1985); **56**, 404(E) (1986).
[19] F. R. Klinkhamer and N. S. Manton, Phys. Rev. D **30**, 2212 (1984); P. Arnold and L. McLerran, *ibid.* **36**, 581 (1987).
[20] A. Dannenberg, Phys. Lett. B **202**, 110 (1988); S. Norimatsu, K. Yamamoto, and A. Tanaka, Phys. Rev. D **35**, 2009 (1987).
[21] E. J. Weinberg and A. Wu, Phys. Rev. D **36**, 2474 (1987).
[22] M. Sher, Phys. Rep. **179**, 273 (1989).
[23] R. Brandenberger, Rev. Mod. Phys. **57**, 1 (1985); A. D. Linde, *ibid.* **42**, 389 (1979); S. Coleman, *Aspects of Symmetry* (Cambridge University Press, Cambridge, England, 1985); R. J. Rivers, *Path Integral Methods in Quantum Field Theory* (Cambridge University Press, Cambridge, England, 1987), pp. 235–288.
[24] I. J. R. Aitchison and C. M. Fraser, Ann. Phys. (N.Y.) **156**, 1 (1984).
[25] S. Coleman and E. Weinberg, Phys. Rev. D **7**, 1888 (1973).
[26] D. A. Kirzhnits and A. D. Linde, Phys. Lett. **42B**, 472 (1972).
[27] D. E. Brahm, in *Baryon Number Violation at the Electroweak Scale,* edited by L. Krauss and S.-J. Rey (World Scientific, Singapore, 1992), p. 130; D. E. Brahm and C. L. Y. Lee, Report No. CALT-68-1881, 1993 (unpublished).
[28] G. Anderson (private communication).
[29] S. Y. Lee and A. M. Sciaccaluga, Nucl. Phys. **B96**, 435 (1975).
[30] R. Jackiw, Phys. Rev. D **9**, 1686 (1974); J. Illiopoulos, C. Itzykson, and A. Martin, Rev. Mod. Phys. **47**, 165 (1975).
[31] H. A. Weldon, Phys. Rev. D **26**, 1394 (1982).
[32] T. S. Evans, Report No. Imperial/TP/91-92/23, 1992 (unpublished).
[33] D. J. Gross, R. D. Pirsarski, and L. G. Yaffe, Rev. Mod. Phys. **53**, 1 (1981); A. D. Linde, Phys. Lett. **93B**, 327 (1980); N. P. Landsman, Physica **A158**, 220 (1989).
[34] A. D. Linde (private communication).
[35] P. Arnold, Phys. Rev. D **46**, 2628 (1992).
[36] L. Dolan and R. Jackiw, Phys. Rev. D **9**, 1686 (1974); **9**, 2904 (1974).
[37] R. Kobes *et al.*, Phys. Rev. Lett. **64**, 2992 (1990); Nucl. Phys. **B355**, 1 (1991).
[38] H. A. Weldon, Phys. Rev. D **28**, 2007 (1983).
[39] P. S. Gribosky and B. R. Holstein, Z. Phys. C **47**, 205 (1990); P. F. Bedaque and A. Das, Phys. Rev. D **45**, 2906 (1992).
[40] B. H. Liu, L. McLerran, and N. Turok, Phys. Rev. D **46**, 2668 (1992).
[41] P. Arnold and O. Espinosa, Phys. Rev. D **47**, 3546 (1993); C. G. Boyd, D. E. Brahm, and S. D. H. Hsu, following paper, Phys. Rev. D **48**, 4963 (1993).
[42] J. R. Espinsosa and M. Quiros, Phys. Lett. B **305**, 98 (1993).
[43] G. W. Anderson, Phys. Lett. B **243**, 265 (1990).
[44] H. Haber and H. A. Weldon, J. Math. Phys. **23**, 1852 (1982).
[45] P. Arnold, E. Braaten, and S. Vokos, Phys. Rev. D **46**, 3576 (1992).